Volume 1 | Number 1 | Jan 2013 | Pages 1–100

Green Chemistry

Cutting-edge research for a greener sustainable future

www.rsc.org/greenchem

Stille couplings in water @RT

ROYAL SOCIETY OF CHEMISTRY

ROYAL SOCIETY OF CHEMISTRY

www.rsc.org/greenchem

Table of Contents Graphic
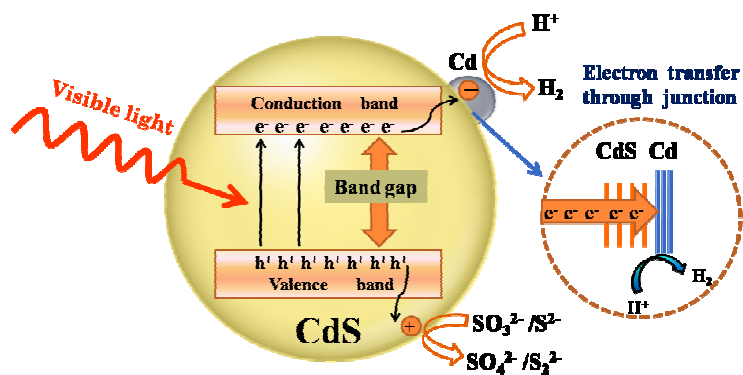
A certain amount of $Na_2S_2O_3 \cdot 5H_2O$ solution added to the solution containing cadmium ion to form Cd/CdS photocatalysts could not only effectively remove cadmium ion but also produce hydrogen efficiently under visible light irradiation.

ARTICLE TYPE

Photochemical preparation of Cd/CdS photocatalysts and its efficient photocatalytic hydrogen production under visible light irradiation

Qizhao Wang*[a], Jiajia Li[a], Yan Bai[a],JuhongLian[a], Haohao Huang*[b], Zhimin Li[a], Ziqiang Lei*[a],Wenfeng Shangguan[c]

Metal Cd can serve as analogues of cocatalyst loaded on CdS to separate electrons and holes to significantly enhance the efficiency of CdS photocatalytic hydrogen production. A series of Cd/CdS photocatalysts were synthesized at various molar ratios of $CdSO_4$
_10 and $Na_2S_2O_3·5H_2O$ in the presence of simulated solar irradiation. Superior photocatalytic activities relative to that of pure CdS were observed on the Cd/CdS photocatalysts. When the optimal molar ratio R of $Na_2S_2O_3·5H_2O$ to cadmium salt is 7, it results in a high average H_2-production rate of 1753 μmol/h. Possible mechanisms for both the formation and the enhanced photocatalytic activity of Cd/CdS were proposed on the basis of
_15 theoretical speculation and experimental observations. Most of all, this work highlights that (i) Cd/CdS leads to an improvement in the photocatalytic activity for H_2 generation; and (ii) adding $Na_2S_2O_3·5H_2O$ into the solution containing cadmium ions to prepare Cd/CdS can effectively remove cadmium ion.

_20 1. Introduction

Increasing awareness of the importance of energy crisis and environmental pollution has stimulated great progresses in the development of green renewable energy. Hydrogen has been regarded as a potential fuel for renewable energy. Photocatalytic
_25 water decomposition into hydrogen is avaluable approach to utilize solar energy.[1-4] Heretofore, photocatalytic hydrogen generation from water on semiconductors has attracted increasing attention and developed rapidly.[5-9] In particular, CdS is one of photocatalysts which is followed with great interests at present.
_30 CdS is one of the most important II–VI semiconductors with a direct bulk phase band gap (2.4 eV) that corresponds well with the electromagnetic spectrum of solar radiation, and also it has the advantage of more negative conduction band edge compared to the H^+/H_2 redox potential.[10,11] In the light irradiation, the
_35 photoinduced charge separation upon excitation occurs in CdS. The electrons and holes are generated in the conduction band (CB) and valence band (VB) of the semiconductor, respectively. But in the photocatalyst CdS, generation of recombination sites between photogenerated electrons and holes is more or less inevitable.[12,13]
_40 There have been many efforts to find alternative ways to separate electrons and holes of CdS in order to make it more efficient in visible light absorption. The cocatalysts loaded on semiconductor photocatalysts can enable or increase the photocatalytic activities of the photocatalysts. In these
_45 photocatalytic reactions, cocatalysts play a key role in the production of H_2, because they can delay the electron hole pair recombination. Moreover, cocatalysts offer low activation

potentials for H_2 evolution and often serve as the active sites to suppress the back reaction of water formation from the evolved
_50 H_2. Some researchers have reported the semiconductor CdS[14,15] and its heterogeneous photocatalysis such as CdS-Pt nanorod heterostructures[16], Ag-doped CdS nanoparticles,[17,18] Core-Shell Au-CdS Nanocrystals,[19] and Pt–PdS/CdS photocatalyst.[20,21] When the metal cocatalyst loads on semiconductor materials, a
_55 Schottky barrieris formed between the two, which acts as an efficient electron trap to prevent photogenerated electron-hole recombination. Consequently, it will result in higher photocatalytic activity for hydrogen production. Herein, we report that metal Cd serves as analogues of cocatalyst loaded on
_60 CdS for photocatalytic H_2 production using sulfide and sulfite as sacrificial reagents under visible light. We found that the activity of CdS could be significantly increased by introducing metal Cd.

What's more, cadmium belongs to the very hazardous heavy metal group, and it can affect a variety of cellular roles, such as
_65 proliferation, apoptosis, differentiation, cell signaling, and gene expression.[22] Because of the risk to human health and a variety of environmental problems,[23,24] the heavy metal pollution has attracted intensive attention. Therefore, the control against heavy metal pollution is an important issue to tackle throughout the
_70 world. In order to create a healthy and good life for mankind, many methods have been employed for treatment of cadmium containing wastewater and polluted earth.[25-30] Herein, we thought that a certain amount of $Na_2S_2O_3 • 5H_2O$ solution was added to the solution containing cadmium ion to form Cd/CdS
_75 photocatalysts,[31] so that it could effectively remove cadmium ion. Therefore, this is a green and effective way of controlling the pollution of heavy metals. We put forward a new method to

reclaim valuable raw materials from industrial wastewater and it will have a good application prospect. In our present work, we demonstrated a facile and rapid method to synthesize Cd/CdS photocatalysts using the solution containing $CdSO_4$ and
5 $Na_2S_2O_3 \cdot 5H_2O$ in the presence of simulated solar irradiation at room temperature. It could not only effectively remove cadmium ion but it was able to produce hydrogen efficiently under visible light irradiation.

10 ## 2.   Experimental

2.1. Preparation of Cd/CdS photocatalysts

All starting materials and reagents were commercially available and used without further purification. In a typical synthesis, a 40 ml solution containing 0.15 M $CdSO_4 \cdot 8/3H_2O$ and 1.2 M
15 $Na_2S_2O_3 \cdot 5H_2O$ in a beaker was used as precursor under vigorous stirring for 20 min and by sonication for 30 min. The beaker is then placed under a simulated solar lamp (Aulight, CEL- HXF300) and kept stirring. When the lamp is turned on, a photochemical reaction takes place. A gray-yellow precipitate is
20 slowly generated with the reaction time in the presence of simulated solar irradiation at room temperature. After 24 h, the gray-yellow precipitate composed of Cd and CdS had formed over the whole solution. We varied the molar ratio of $Na_2S_2O_3 \cdot 5H_2O$ to cadmium salt, represented as R, from 5 to 10
25 while keeping the $CdSO_4$ concentration fixed. When Cd/CdS were put into 0.1 M nitric acid, pure CdS formed after several minutes. Finally, the resulting Cd/CdS photocatalysts were centrifuged and subsequently washed with deionized water and ethanol, then dried in vacuum at 60 ^oC for 8 h.

30 ### 2.2. Photocatalytic activity

About 0.15 g of Cd/CdS photocatalyst powders was dispersed in 100 mL of aqueous solution containing 0.5 M Na_2S and 0.5 M Na_2SO_3 as the sacrificial reagents in the reactor under the vertical
35 irradiation of a 300 W Xe lamp. The suspension was then thoroughly degassed and irradiated by a 300 W Xe lamp (Aulight, CEL-HXF300) which is equipped with an optical filter (0.1 M $NaNO_2$ aqueous solution) to cut off the light in the ultraviolet region. The amounts of H_2 evolution were measured by using a
40 gas chromatography (QC-9101, 5Å-column) with thermal conductivity detector (TCD) and Ar as carrier gas.

2.3. Characterization

X-ray diffraction patterns (XRD) of the prepared metal oxides
45 were recorded on a Rigaku X-ray diffractometer D/MAX-2200/PC equipped with Cu K α radiation(40 kV, 20 mA). Scanning electron microscopy (SEM) images were obtained using JSM-6701F. UV–vis diffuse reflectance spectra were measured using Shimadzu UV-3100 spectrophotometer. The
50 reflectance spectra were transformed to absorption intensity by using Kubelka–Munk method. X-ray photoelectron spectroscopic (XPS) characterizations were performed on PHI5702 photoelectron spectrometer. Binding energy was referred to C 1s (284.80 eV). Nitrogen adsorption-desorption isotherms and the
55 Brunauer-Emmett-Teller (BET) surface areas were collected at 77

K on a TriStar II 3020 system. Steady and time-resolved fluorescence emission spectra were recorded at room temperature with a fluorescence spectrophotometer (PE, LS-55).

60 ## 3.   Results and discussion

3.1. Cd/CdS   photocatalysts   structure   and   optical characterization
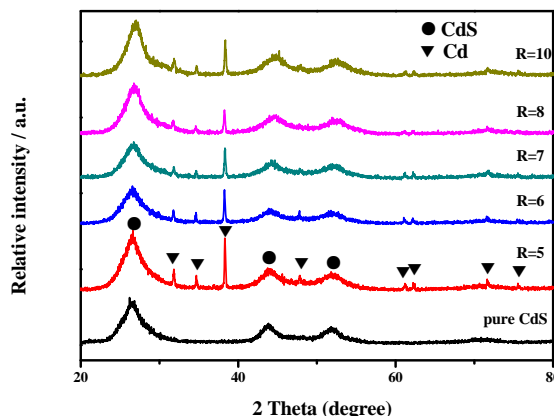

Fig. 1 XRD patterns of the as-synthesized Cd/CdS photocatalysts with
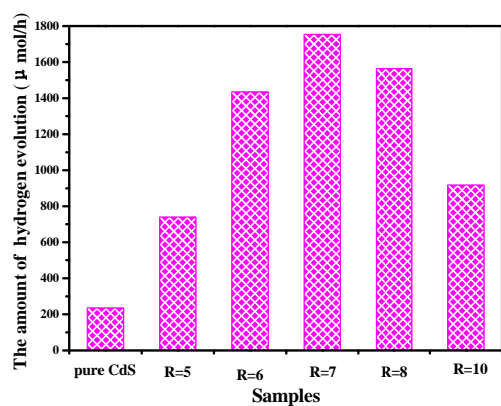65 different R values.

Fig.1 shows the X-ray diffraction (XRD) patterns of the pure CdS and Cd/CdS photocatalysts with different R values. It can be seen that the as-prepared serial Cd/CdS photocatalysts possess
70 similar XRD patterns. All of these samples give rise to diffraction peaks of hawleyite CdS phase with lattice constant a = 5.818 Å (JCPDS No. 10-0454). The main diffraction peak positions of the obtained products appear at 26.53^o, 43.95^o and 51.95^o, which correspond to the (111), (220), and (311) crystal faces of CdS,
75 respectively. Peaks at 31.79^o, 34.67^o, 38.27^o and others show the existence of metallic cadmium (JCPDS No. 65-3363). These diffraction peaks of CdS and metallic cadmium are consistent with the previous report.[32] Obviously, upon further increase of the content of $Na_2S_2O_3 \cdot 5H_2O$, the main diffraction peak positions
80 of metallic cadmium decreases, indicating it was probably that the content of metallic cadmium decreased along with increasing amount of $Na_2S_2O_3 \cdot 5H_2O$.
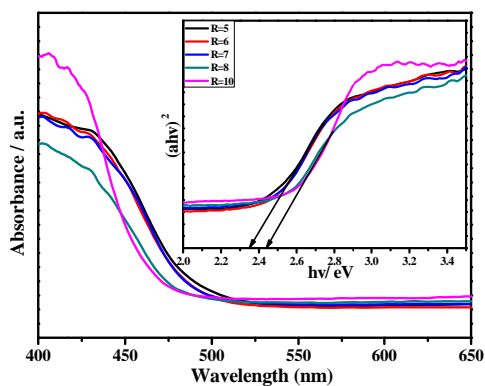
Fig. 2 UV-Vis diffuse reflectancespectra of samples.The inset isband gap evaluation from the plots of $(\alpha h\nu)^2$ versus photon energy (hv).

The UV-Vis diffuse reflectance absorption spectra of Cd/CdS
5 photocatalysts at various values of R are shown in Fig. 2. All these spectra are recorded in the wavelength range of 400-650 nm. Interestingly, with increasing R value, all these photocatalysts show almost the same absorption profile with a steep absorption edge in 450-500 nm, which is independent of the R values.
10 Because of the characteristic of the absorption peaks of Cd/CdS photocatalysts mentioned above, it is difficult to estimate the photocatalytic activity of Cd/CdS photocatalysts for hydrogen evolution from UV-Vis diffuse reflectance spectra.[33] After comparison, we find a small red-shift for the samples, which
15 indicates that there is a decrease in energy band gap of these samples. The direct band gap values of the samples were estimated from the $(\alpha h\nu)^2$ versus photon energy (hv) plot (insert of Fig. 2) . When the R value is equal to 5, 6 and 7, the band gaps of the samples are approximately equal and are estimated to be
20 2.35 eV, which is lower than that for R= 8 and 10 (2.42 eV). It indicates that these samples have greater carrier concentration, since the optical absorption in this wavelength region is due to free-carrier absorption of the conduction electrons. Thus, it is speculated that these samples may have a higher photocatalytic
25 activity.

3.2. Photocatalytic activity

40

Fig. 3 shows H$_2$ evolution on Cd/CdS photocatalysts at various values of R under visible light. Metallic cadmium exhibited a significant influence on the photocatalytic activity. For pure CdS alone, a relatively low photocatalytic H$_2$-production rate is
195 observed as expected due to the rapid recombination of conduction band (CB) electrons and valence band (VB) holes. In the presence of an amount of metallic cadmium, the activity of sample Cd/CdS (R=5) is slightly enhanced to 740 μmol/h. When R becomes 7, the average H$_2$-production rate reaches the
200 maximum value of 1753 μmol/h, nearly 7.5 times of that for pure CdS, and the H$_2$-production rate is significantly greater than that of most semiconductor photocatalysts. There is a main reason why the photocatalytic activity of the serial Cd/CdS photocatalystsis higher than that of CdS: Cd serves as an acceptor
205 and transfers channels of the electrons generated in the CdS semiconductor, so it effectively decreases the recombination probability of the photoexcited electron hole pairs, leaving more charge carriers to form reactive species. The results indicate that the photocatalytic activity of CdS photocatalysts is improved by
210 the introduction of Cd. With ICP tests we found out when the R value is 5, 6, 7, 8 and 10, the content of Cd is 53.02%, 46.63%, 37.11%, 40.8% and 41.61%, respectively. However, the rate of H$_2$ evolution first increases with increasing the value of R up to 7 and then decreases. In particular, when R value reaches 10, the
215 photocatalytic activity dramatically decreases, with an average H$_2$-production rate of 917 μmol/h. This is probably because the surplus Cd can work as an optical filter to shield incident light, hence suppressing further enhancement of photocatalytic activity for hydrogen evolution. As a consequence, a suitable content of
220 Cd is crucial for optimizing the photocatalytic activity of Cd/CdS photocatalysts.
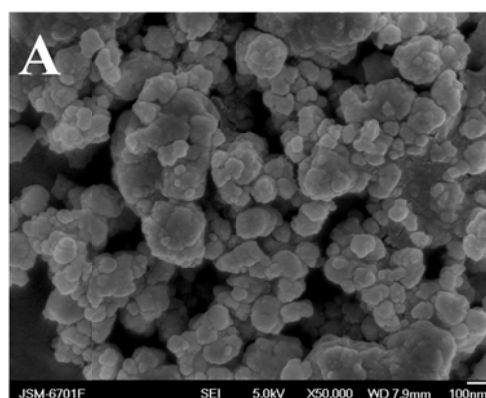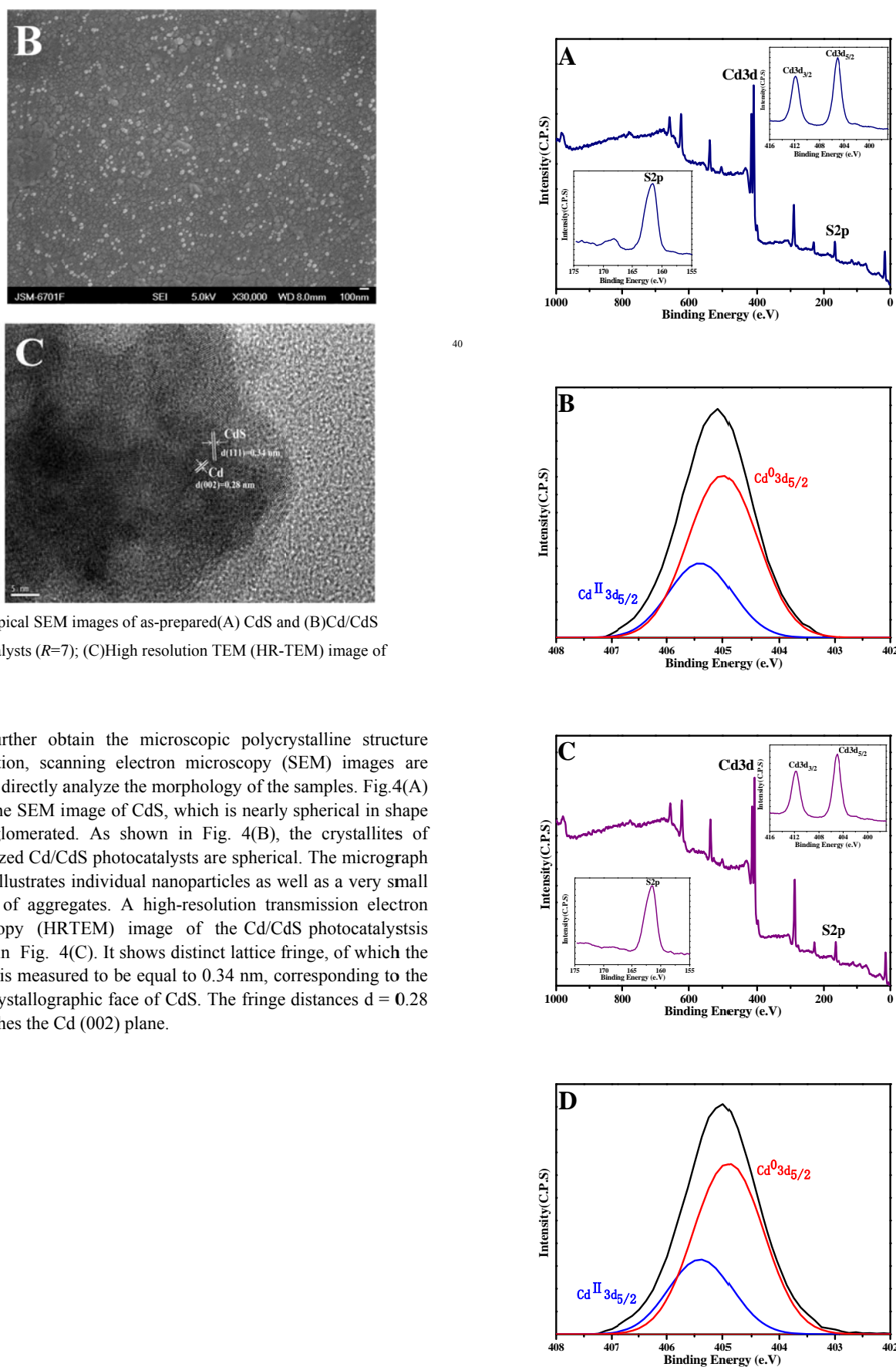
Fig. 4 Typical SEM images of as-prepared(A) CdS and (B)Cd/CdS photocatalysts (*R*=7); (C)High resolution TEM (HR-TEM) image of Cd/CdS.

To further obtain the microscopic polycrystalline structure information, scanning electron microscopy (SEM) images are taken to directly analyze the morphology of the samples. Fig.4(A) shows the SEM image of CdS, which is nearly spherical in shape and agglomerated. As shown in Fig. 4(B), the crystallites of synthesized Cd/CdS photocatalysts are spherical. The micrograph clearly illustrates individual nanoparticles as well as a very small number of aggregates. A high-resolution transmission electron microscopy (HRTEM) image of the Cd/CdS photocatalystsis shown in Fig. 4(C). It shows distinct lattice fringe, of which the spacing is measured to be equal to 0.34 nm, corresponding to the (111) crystallographic face of CdS. The fringe distances d = 0.28 nmmatches the Cd (002) plane.

Fig. 5 XPS spectra of the Cd/CdS (R=7) photocatalysts: (A) and (B) before reaction; (C) and (D) after reaction.

The binding energies of electrons determined by X-ray photoemission spectroscopy (XPS) provide useful information of
5 the Cd/CdS photocatalysts(R=7) before and after photocatalytic reaction(Fig. 5). The strong cadmium peak and sulfur peak are found in the spectra. The binding energy corresponding to Cd $3d_{3/2}$ and $3d_{5/2}$ is 411.8 eV and 405.3 eV, and the distinct peak of S_{2p} at 161.7 eV corresponds to S^{2-} of CdS nanoparticles, which is
10 in agreement with the literatures.[34,35] Furthermore, the atomic concentration of cadmium and sulfur can be calculated based on the peak area.[32] Cd/CdS(R=7) shows the contents of Cd and S elements are 65.1 at% and 34.9 at% before reaction, while 65.3% Cd and 34.7% S for Cd/CdS after reaction. It can be concluded
15 that molar proportion of Cd/CdS is equal to 0.86:1 and 0.88:1 before reaction and after reaction, respectively. In Fig. 5(B) and (D), the Cd $3d_{5/2}$ region displays the Cd^{II} $3d_{5/2}$ (405.4eV) and Cd^0 $3d_{5/2}$ (405eV) peaks, which confirmed the presence of both Cd^{2+} and Cd^0. In addition, the relative peak area of Cd^{2+} and Cd^0 of the
20 photocatalyst Cd/CdS can be quantified. The molar ratio of Cd^{2+} and Cd^0 is 0.422 and 0.403 before reaction and after reaction, respectively.
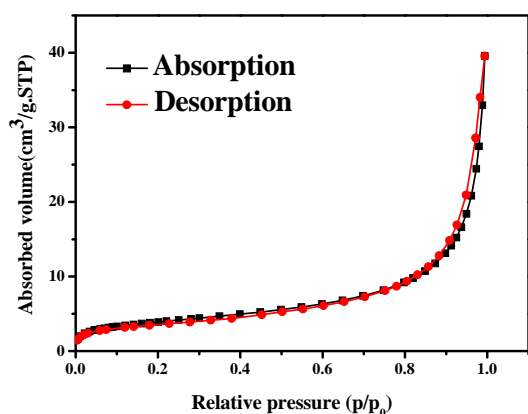

Fig. 6 BET adsorption-desorption isotherms of Cd/CdS (R=7).

25 The N_2 adsorption-desorption isotherm of the Cd/CdS(R=7) photocatalysts is depicted in Fig. 6. Specific surface area of the sample is approximately 14 m^2g^{-1}.

A recycling of photocatalytic hydrogen evolution on the Cd/CdS(R=7) was invesigated to evaluate photocatalytic stability
30 during a long-term photocatalytic reaction (Fig. 7(A)). In order to examine the reproducibility of the photocatalytic material and remove the dissolved gases, in every 2.5 h of reaction the reactor was evacuated and the photocatalytic experiment was repeated. For evaluating the photostability of the photocatalyst, the
35 Cd/CdS(R=7) after the first run was picked out from the sacrificial reagent solution, washed with distilled water, and then dried at 80 °C . The same photocatalyst was used for the second and third run of the photochemical reaction under the same conditions. The activity was found to be almost the same in three
40 repeated runs. Fig. 7(A) shows a typical reaction time course for H_2 evolution from an aqueous Na_2SO_3/Na_2S solution over Cd/CdS(R=7) under visible-light irradiation (λ > 400 nm). The initial H_2-production rate reached 955 μmol/h. In the next run, the rate of hydrogen evolution mildly declined. However, the

45 hydrogen evolution rate still remained 847 μmol/h after the third run reaction. The decrease in the rate of hydrogen evolution might be related to the deactivation of the photocatalyst or attributed to the consumption of the sacrificial reagents in the solution.[37] Control experiments indicated that no appreciable
50 hydrogen production was detected in the dark, suggesting that hydrogen was produced by photocatalytic reactions on the photocatalyst under visible-light irradiation. After the photocatalytic reaction, we collected the photocatalyst powders and washed with distilled water for several times. Then, the
55 corresponding XRD patterns of the photocatalysts before and after the photocatalytic reaction in Fig. 7(B) have no notable differences. It proved that the photocatalyst was stable enough during the reaction.
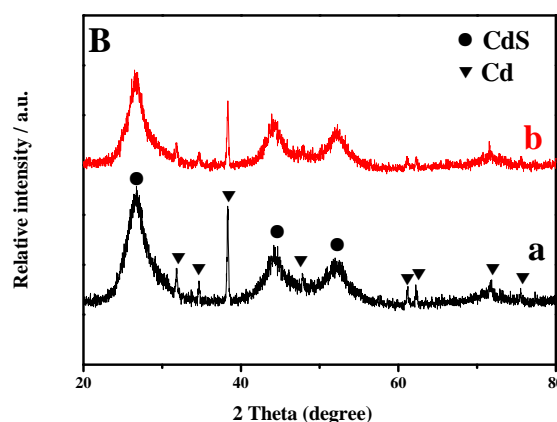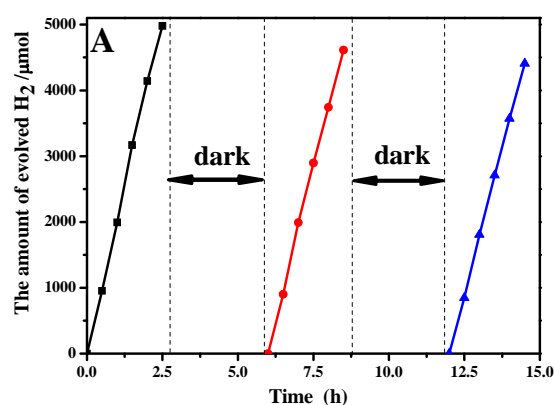

60 **Fig. 7** (A) A test of the stability of the Cd/CdS(R=7) photocatalysts for photocatalytic hydrogen production. (B) XRD patterns of the Cd/CdS photocatalysts (R=7): (a) before reaction and (b) after reaction.
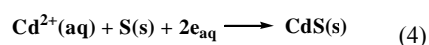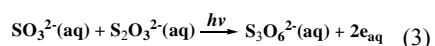
Photoluminescence (PL) analysis was employed to investigate
65 the migration, transfer and separation efficiencies of photo-generated electrons and holes in semiconductors, since PL emission of semiconductor mainly arises from the charge carrier recombination. Fig.8 shows the room temperature photoluminescence spectra of pure CdS and Cd/CdS
70 photocatalysts with an excitation wavelength of 650 nm. This PL band is a sulfur vacancy related emission which is generally attributed to the recombination of an electron trapped in a sulfur vacancy with a hole in the valance band of CdS.[38] The Cd/CdS photocatalysts give a similar band-to-band fluorescence emission

characteristic as pure CdS. Clearly, the photocatalytic activity of CdS can be substantially improved by introducing Cd. Much weakened emission intensity of Cd/CdS compared to pure CdS, however, suggests decreased recombination probability of
5 photoexcited charge carriers in the Cd/CdS photocatalysts.
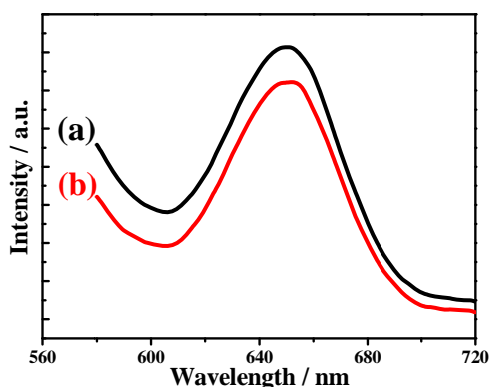
Fig. 8 Fluorescence emission spectra of (a) pure CdS and (b) Cd/CdS photocatalysts (*R*=7).

On the basis of the above results, the probable mechanism for
10 the formation of Cd/CdS photocatalysts has been reported.[31,32] The serial Cd/CdS photocatalysts were synthesized at room temperature using the solution composed of $CdSO_4$ and $Na_2S_2O_3 \cdot 5H_2O$ in the presence of simulated solar irradiation. When simulated solar irradiated the precursor, a series of
15 photochemical reactions occurred.[39] The $S_2O_3^{2-}$ ions served as the source of sulfur, and it was supposed to adsorb photons and dissociate to provide sulfur under irradiation. Meanwhile, $S_2O_3^{2-}$ ions provide aquated electrons, which could cause the formation of CdS:

20

$$S_2O_3^{2-}(aq) \xrightarrow{h\nu} S(s) + SO_3^{2-} \qquad (1)$$

$$2S_2O_3^{2-}(aq) \xrightarrow{h\nu} S_4O_6^{2-}(aq) + 2e_{aq} \qquad (2)$$

$$SO_3^{2-}(aq) + S_2O_3^{2-}(aq) \xrightarrow{h\nu} S_3O_6^{2-}(aq) + 2e_{aq} \qquad (3)$$

$$Cd^{2+}(aq) + S(s) + 2e_{aq} \longrightarrow CdS(s) \qquad (4)$$
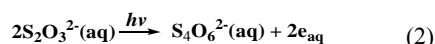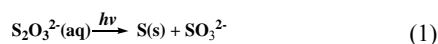
25 The reduction potential of S(s) has a relatively low value ($E^0_{S/S^{2-}}$ = -0.445V vs.SHE), whereas the aquated electrons is a strong reductant.[40] The electrons could unite with Cd^{2+} to generate metallic cadmium, and then react with S(s) to form CdS(reaction(4)).

30 By the same argument, Cd^{2+} ($E^0_{Cd^{2+}/Cd}$ = -0.4022V vs. SHE) could be reduced to metallic cadmium and CdS could form immediately after S(s) reacted with metallic cadmium as follows

$$Cd^{2+}(aq) + 2e_{aq} \longrightarrow Cd(s) \qquad (5)$$

$$Cd + S \longrightarrow CdS(s) \qquad (6)$$
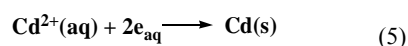
45 In the reaction (6), the Gibbs free energy can be calculated as:[32]

$$\triangle_r G^0_m = -440.70 - 0.15T (kJ\ mol^{-1}) < 0$$

There is no doubt that it is a thermodynamically favored reaction. It is therefore reasonable to conclude that CdS and
75 metallic cadmium could form by the previously mentioned three mechanisms (reactions (4), (5) and (6)). In the reactions (4) and (6), sulfur would combine with Cd^{2+} or metallic cadmium to generate CdS(s). And the photo-generated electrons bond with Cd^{2+} to form metallic cadmium(reaction (5)).

75 Nevertheless, the sulfur from the photodegradation of $S_2O_3^{2-}$ possesses high activity and may be oxidized by oxygen during CdS formation due to its exposure to air. It would leave more photo-generated electrons to react with Cd^{2+}. This leads to an enrichment of cadmium(reaction (5)) in the products and a
80 deficiency of sulfur(reaction (7)).

$$S + O_2 \longrightarrow SO_2 \qquad (7)$$
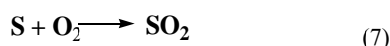
As a result, Cd and CdS crystal nuclei absorbed the corresponding ions and grew gradually to form a Cd/CdS
70 nanocomposite.
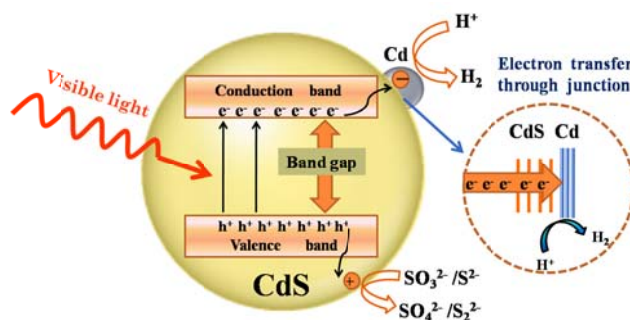
Fig. 9 Schematic illustration of photo-generated charge transfer process for photocatalytic hydrogen evolution over the Cd/CdS photocatalysts from an aqueous solution containing Na_2SO_3/Na_2S under visible-light
80 irradiation.

Furthermore, the proposed mechanism of charge transfer in the case of the serial Cd/CdS photocatalysts can be illustrated by the schematic of Fig. 9. It has been reported that CdS is an n-type semiconductor with a band gap of 2.4 eV.
160 When loaded with metal Cd, it was found that the rate of H_2 production was greatly enhanced. This was attributed to the fact that the Schottky barrier formed at the metal and CdS interface could serve as an efficient electron trap which prevents photogenerated electron-hole recombination. The effect of the
165 nature of the metal was interpreted in terms of different electronic interactions between the metal nanoparticles and the CdS surface. It was also reported that the smaller the Schottky barrier height at the metal/semiconductor junction, the greater the electron flow from semiconductor to metal, thus leading to higher
170 photocatalytic activity for hydrogen production.[7] Consequently, the Cd particles deposited on the surface of the CdS particles are necessary to ensure a good electron transfer. Cd acting as analogues of cocatalyst is supposed to be beneficial for the efficient separation and transfer of the photoexcited electrons and

holes. In the present work, photocatalytic H$_2$-production activity of the prepared Cd/CdS photocatalysts was evaluated under visible-light irradiation using an aqueous Na$_2$SO$_3$/Na$_2$S solution as a sacrificial reagent and Cd acted like cocatalyst. The sacrificial reagent can prevent sulfide photocatalysts from the photocorrosion by providing sacrificial electron donors to consume the photogenerated holes, and Cd can reduce the overpotential in the production of H$_2$ from water and suppress the fast backward reaction as well.

Conclusions

A series of Cd/CdS photocatalysts with various molar ratios of Na$_2$S$_2$O$_3$ • 5H$_2$O to CdSO$_4$ were successfully synthesized. Cd as analogues of cocatalyst introduced in the preparation of CdS was demonstrated as an efficient visible light ($\lambda > 400$ nm) responsive photocatalyst for hydrogen evolution in photocatalytic water splitting reaction. The experimental results showed that most of Cd/CdS photocatalysts had higher photocatalytic activity than pure CdS because of effective photoexcited electron hole pair separation. In addition, the reaction time and stability of the composite photocatalyst was enhanced a lot. Through this research we found that Cd had great influence on the photocatalytic activity of CdS, which could effectively prohibit the recombination of photogenerated electrons and holes and play an important role in the highly active photocatalysts for solar energy conversion. In summary, our experimental results demonstrated that a certain amount of Na$_2$S$_2$O$_3$ • 5H$_2$O solution added to the solution containing cadmium ion to form Cd/CdS photocatalysts could not only effectively remove cadmium ion but also produce hydrogen efficiently under visible light irradiation. Furthermore, this approach is a green and effective way to control the pollution of heavy metals. We put forward a new method to reclaim valuable raw materials from industrial wastewater, and it will have a good application prospect.

Acknowledgements

Notes and references

aCollege of Chemistry and Chemical Engineering, Northwest Normal University, Key Laboratory of Eco-Environment-Related Polymer Materials, Ministry of Education of China, Key Laboratory of Gansu Polymer Materials, Lanzhou 730070, China
bCollege of Materials Science and Engineering, South China University of Technology, Guangzhou, 510640, China
cResearch Center for Combustion and Environment Technology, Shanghai Jiao Tong University, Shanghai 200240, China

Fax: +86 931 7975521;Tel: +86 931 7972677.
E-mail: wangqizhao@163.com;
qizhaosjtu@gmail.com(Q. Wang)
scuthhh@hotmail.com(H. Huang),
leiziqiang@hotmail.com (Z. Lei)

1. K. Maeda, K. Teramura, D. Lu, N. Saito, Y. Inoue and K. Domen, *Angew. Chem. Int. Ed.*, 2006, **118**, 7970-7973.
2. K. Maeda, K. Teramura, D. Lu, N. Saito, Y. Inoue and K. Domen, *Nature*, 2006, **440**, 295 .
3. A. Kudo and Y. Miseki, *Chem. Soc. Rev.*, 2009, **38**, 253-278.
4. X. Chen, S. Shen, L. Guo and S. S. Mao, *Chem. Rev.*, 2010, **110**, 6503-6570.
5. Z. Lei, W. You, M. Liu, G. Zhou, T. Takata, M. Hara, K. Domen and C. Li, *Chem.Commun.*, 2003, **17**, 2142-2143.
6. Y.K. Kim, H. Park, *Appl. Catal. B: Environmental*, 2012,**125**, 530-537.
7. J. Y. Shi, J. Chen, Z. C. Feng, T. Chen, Y. X. Lian, X. L. Wang and C. Li, *J. Phys. Chem. C*, 2007, **111**, 693-699.
8. I. S. Cho, D. W. Kim, S. Lee, C. H. Kwak, S. T. Bae, J. H. Noh, S. H. Yoon, H. S. Jung, D. W. Kim and K. S. Hong, *Adv. Funct. Mater.*, 2008, **18**, 2154-2162.
9. Q. Z. Wang, H. Liu, J. Yuan and W. F. Shangguan, *Catal.Lett.*, 2009, **131**, 161-163.
10. Q. Z. Wang, N. An, W. Chen, R. F. Wang, F. P. Wang, Z. Q. Lei and W. F. Shangguan, *Int. J. Hydrogen Energy.*, 2012, **37**, 12886-12892.
11. Z. Jindal and N. K. Verma, *Physica E.*,2009, **41**,1752-1756.
12. Q. Li, B. D. Guo, J. G. Yu, J. G. Ran, B. H. Zhang, H. J. Yan and J. R. Gong, *J. Am. Chem. Soc.*, 2011, **133**,10878-10884.
13. P. S. Lunawat, S. Senapati, R. Kumar and N. M. Gupta, *Int. J. Hydrogen Energy.*, 2007, **32**, 2784-2790.
14. H. M. Yang, C. H. Huang, X. W. Li, R. R. Shi and K. Zhang, *Mater. Chem. Phys.*, 2005, **90**, 155-158.
15. D. Xu, K. K. Sushil and W. L. Deng, *Sep. Purif. Technol.*, 2009, **68**, 61-64.
16. K. F. Wu, H. M. Zhu, Z. Liu, W. Rodrguez-Cordoba and T. Q. Lian, *J. Am. Chem. Soc.*, 2012, **134**, 10337-10340.
17. J. Ma, G. A. Tai and W. L. Guo, *Ultrason. Sonochem.*, 2010, **17**, 534-540.
18. A. Kumar and V. Chaudhary, *J. Photochem. Photobiol. A: Chemistry.*, 2007, **189**, 272-279.
19. T. T. Yang, W. T. Chen, Y. J. Hsu, K. H. Wei, T. Y. Lin and T. W. Lin, *J. Phys. Chem. C*, 2010, **114**, 11414-11420.
20. H. J. Yan, J. H. Yang, G. J. Ma, G. P. Wu, X. Zong, Z. B. Lei, J. G. Shi and C. Li, *J. Catal.*,2009, **266**,165-168.
21. H. J. Yan, J. H. Yang, X. L. Wang, F. Y. Wen, Z. J. Wang, D. Y. Fan, J. Y. Shi and C. Li, *J. Catal.*,2012, **290**, 151-157.
22. M. F. Philips, A.I.Gopalanb and K.P.Lee.*J. Hazard. Mater.*,2012,**237-238**,46-54.
23. S. S. Mao and X. Chen, *Int. J. Energy Res.*, 2007, **31**, 619-636.
24. T. N. Veziroḡlu and S. Sxahin, *Energy Convers. Manage.*, 2008, **49**, 1820-1831.
25. A. Jang, Y. W. Seo and P. L. Bishop, *Environ. Pollut.*, 2005, **133**, 117-128.
26. S. G. Alonso, M. Catalá, R. R. Maroto, J. L. R. Gil, A. G. Miguel and Y. Valcárcel, *Environ. Int.*, 2010, **36**, 195-201.
27. M. R. Hoffmann, S. T. Martin, W. Y. Choi and D. W. Bahnemann, *Chem. Rev.*, 1995, **95**, 69-96.
28. Y. Zhi, Y. G. Li, Q. H. Zhang and H. Z. Wang, *Langmuir*, 2010, **26**, 15546-15553.
29. J. G. Yu and X. X. Yu, *Environ. Sci. Technol.*, 2008, 42, 4902-4907.
30. Y. Liu, L. Yu, Y. Hu, C. F. Guo, F. M. Zhang and X. W. Lou,*Nanoscale*, 2012, **4**, 183-187.
31. Y. Y. Huang, F. Q. Sun, H. J. Wang, Y. He, L. S. Li, Z. X. Huang, Q. S. Wu and J. C. Yu, *J. Mater. Chem.*, 2009, **19**, 6901-6906.
32. Z. X. Huang, F. Q. Sun, Y. Zhang, K. Y. Gu, X. Q. Zou, Y. Y. Huang, Q. S. Wu and Z. H. Zhang, *J. Colloid Interface Sci.*, 2011, **356**,783-789.
33. K. He, M. T. Li and L. J. Guo, *Int. J. Hydrogen Energy.*, 2012, **37**, 755-759.
34. N. Biswal, D. P. Das, S. Martha and K. M. Parida, *Int. J. Hydrogen Energy*, 2011, **36**, 13452-13460.

35. Q. Li, B. D. Guo, J. G. Yu, J. R. Ran, B. H. Zhang, H. J. Yan and J. R. Gong, *J. Am. Chem. Soc.*, 2011, **133**, 10878-10884.

36. Y. X. Li, G. Chen, Q. Wang, X. Wang , A. K. Zhou and Z. Y. Shen,*Adv. Funct. Mater.*, 2010, **20**, 3390-3398.

5 37. Y. Liu, L. Zhou, Y. Hu, C. F. Guo, H. S. Qian, F. M. Zhang, X. W. Lou, *J. Mater. Chem.*, 2011, **21**,18359-18364.

38. Y. Hu, X. H. Gao, L. Yu, Y. R. Wang, J. Q. Ning, S. J. Xu, X. W. Lou. *Angew. Chem. Int. Ed.*,2013, **52**, 5636 –5639.

39. Y. Hu, H. H. Qian, Y. Liu, G. H. Du, F. M. Zhang, L.B. Wang, X. Hu,
10   *Cryst. Eng. Comm.*, 2011, **133**, 3438-3443.

40.Y. Liu, Y. Hu, M. J. Zhou, H. S. Qian, X. Hu, *Appl. Catal. B: Environmental.*, 2012, **125**, 425-431.